Contribution from the Departments of Chemistry, Middle East Technical University, 06531 Ankara, Turkey, and Northern Illinois University, DeKalb, Illinois 60115

Electronic Absorption and Magnetic Circular Dichroism Spectra for Binuclear $Pt_2(SO_4)_4X_2^{n-}$ and $Pt_2(HPO_4)_4X_2^{n-}$ Ions in Aqueous Solution

Gülsün Gökagac,[†] Hüseyin Isci,*[,†] and W. Roy Mason*[,‡]

Received December 2, 1991

Electronic absorption and 7-T magnetic circular dichroism (MCD) spectra in the UV-visible region are reported for the binuclear diplatinum(III) ions: $Pt_2(SO_4)_4X_2^{n-}$, $n = 2$, $X = H_2O$, NH_3; $n = 4$, $X = Cl^-$, Br^-, OH^-. $Pt_2(HPO_4)_4X_2^{n-}$, $n = 2$, $X = H_2O$, Me_2S; $n = 4$, $X = Cl^-$, Br^-. Both the absorption spectra and the MCD spectra for complexes with the same axial ligand X are similar for oxo-bridging SO_4^{2-} or HPO_4^{2-}. However, the MCD spectra show marked differences depending upon the nature of the X ligand. The most intense absorption band observed in the UV for the diaqua complexes at 4.4 μm^{-1} exhibits a negative *A* term, while that for the dichloro complexes at 3.3 μm^{-1}, or for the dibromo complex at 2.95 μm^{-1}, shows a positive *A* term. The intense bands in the spectra of the Me_2S complex at 2.96 μm^{-1}, the NH_3 complex at 3.84 μm^{-1}, and the OH^- complex at 3.62 μm^{-1} show positive *B* terms. The absorption and MCD spectra are interpreted in terms of ligand to metal change transfer (LMCT) from bridge oxygens for the diaqua complexes and in terms of π LMCT from the axial halide ligands for the dihalo complexes. The intense bands for the Me_2S, NH_3, and OH^- complexes are ascribed to $(X\sigma, d\sigma) \rightarrow d\sigma^*$ excitation. For each type of complex a lower energy, less intense band system is also observed. This system is not very strongly dependent upon the nature of X and is assigned as $d\pi^* \rightarrow d\sigma^*$ or σ^*PtO_4 (predominantly $d_{x^2-y^2}$).

Introduction

Binuclear diplatinum(III) complexes of the type $Pt_2(B\text{-}B)_4X_2^{n-}$, where B-B is a bidentate bridging ligand and X is a monodentate axial ligand, have structures with essentially D_{4h} symmetry sketched in **1** and feature an intramolecular Pt-Pt bond.[1,2] The

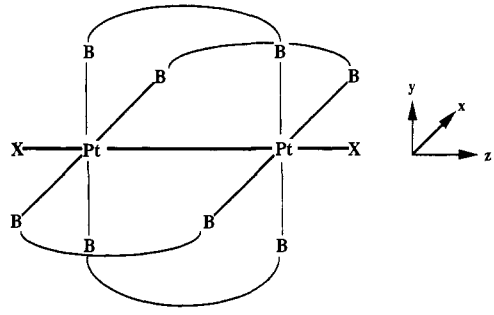

1

conventional description of metal-metal bonding in binuclear transition metal complexes[1,3] applied to the $5d^7$-$5d^7$ overlaps in the Pt_2^{6+} core of **1** assigns the ground-state electron configuration as $(d\sigma)^2(d\pi)^4(d\delta)^2(d\delta^*)^2(d\pi^*)^4$, which gives a diamagnetic single bond. The empty $d_{x^2-y^2}$ orbitals on the Pt atoms, which are also of δ symmetry with respect to the Pt-Pt bond, are strongly involved in B-B-Pt σ bonding and are destabilized to higher energy than the occupied d orbitals. The Pt-Pt bond length in complexes **1** varies from 2.46-2.53 Å for B-B = O-donor HPO_4^{2-} or SO_4^{2-} bridging ligands[1,4] to 2.68-2.78 Å for B-B = P-donor $(PO_2H)_2O^{2-}$ (POP) or $(PO_2H)_2CH_2^{2-}$ (PCP) ligands.[2,5,6] The axial ligands X affect the Pt-Pt bond length slightly, with a longer Pt-Pt distance found for stronger donor ligands. The Pt-X bond length and the rate of replacement of the X ligands vary inversely with the Pt-Pt bond length, with the HPO_4^{2-} complexes ca. 10^4 times more reactive than analogous POP complexes.[7]

The complexes **1** exhibit characteristic intense electronic absorptions in the UV-visible region which have been ascribed to electron promotion to the empty $d\sigma^*$ orbital, the population of which would be expected to weaken the Pt-Pt bond. The most extensively studied complexes have been $Pt_2(POP)_4X_2^{n-}$, where spectral assignments have been based on the interpretation of absorption,[2,6,8,9] emission/excitation,[10] and magnetic circular dichroism (MCD) spectra.[11] An intense UV band which is sensitive to the nature of X has been assigned as $\sigma \rightarrow d\sigma^*$, where the occupied σ level has both $X\sigma$ and $d\sigma$ character in proportion to the donor strength of X and the relative energies of the ligand and 5d Pt orbitals. Two lower energy weaker band systems have been identified as $d\pi^* \rightarrow d\sigma^*$ and $d\delta^* \rightarrow d\sigma^*$. A similar spectral pattern has been observed for $Pt_2(HPO_4)_4X_2^{n-}$ complexes, and a recent discussion of the absorption spectra suggested analogous assignments to the POP complexes.[12] Emission and excitation spectra for $Pt_2(HPO_4)_4X_2^{n-}$, $X = H_2O$, Cl^-, and Br^-, were then reasonably interpreted in terms of emission from spin-orbit states of triplet parentage from the $(d\pi^*)^3(d\sigma^*)$ excited configuration.[12]

As noted above, there are significant differences in Pt-Pt bond length and X ligand reactivity between the $Pt_2(HPO_4)_4X_2^{n-}$ (and presumably also the $Pt_2(SO_4)_4X_2^{n-}$) complexes and analogous $Pt_2(POP)_4X_2^{n-}$ complexes—differences which point to changes in relative Pt-Pt and Pt-X bonding and which would affect the $X\sigma$, $d\sigma$, and $d\sigma^*$ orbitals to a considerable extent. Therefore an assumption of analogous spectral assignments, and the implied similarity in electronic structure which accompanies the assumption, may be questionable without more detailed corroboration. In order to test the assumption, to provide additional spectroscopic data to probe the nature of the Pt-Pt bond, and to characterize the low-energy excited states which perturb the bond, some aqueous solution absorption and MCD spectra were obtained for $Pt_2(HPO_4)_4X_2^{n-}$, $X = H_2O$, Cl^-, Br^-, and Me_2S, and $Pt_2(SO_4)_4X_2^{n-}$, $X = H_2O$, Cl^-, Br^-, OH^-, and NH_3 and are reported herein. The results for these HPO_4^{2-} and SO_4^{2-} complexes reveal some notable differences when compared to the POP complexes

[†] Middle East Technical University.
[‡] Northern Illinois University.

(1) Cotton, F. A.; Walton, R. A. *Struct. Bonding* **1985**, *62*, 1.
(2) (a) Roundhill, D. M.; Gray, H. B.; Che, C.-M. *Acc. Chem. Res.* **1989**, *22*, 55. (b) Zipp, A. P. *Coord. Chem. Rev.* **1988**, *84*, 47.
(3) Cotton, F. A.; Walton, R. A. *Multiple Bonds between Metal Atoms*; Wiley-Interscience: New York, 1982.
(4) Bancroft, D. P.; Cotton, F. A.; Falvello, L. R.; Han, S.; Schwotzer. *Inorg. Chim. Acta* **1984**, *87*, 147.
(5) Che, C.-M.; Lee, W.-M.; Mak, T. C. W.; Gray, H. B. *J. Am. Chem. Soc.* **1986**, *108*, 4446.
(6) Che, C.-M.; Mak, T. C. W.; Miskowski, V. M.; Gray, H. B. *J. Am. Chem. Soc.* **1986**, *108*, 7840.
(7) El-Mehdawi, R.; Bryan, S. A.; Roundhill, D. M. *J. Am. Chem. Soc.* **1985**, *107*, 6282.
(8) Che, C.-M.; Butler, L. G.; Grunthaner, P. J.; Gray, H. B. *J. Am. Chem. Soc.* **1985**, *107*, 4662.
(9) Che, C.-M.; Lee, W.-M.; Cho, K.-C. *J. Am. Chem. Soc.* **1988**, *110*, 5407.
(10) Stiegman, A. E.; Miskowski, V. M.; Gray, H. B. *J. Am. Chem. Soc.* **1986**, *108*, 2781.
(11) Isci, H.; Mason, W. R. *Inorg. Chem.* **1985**, *24*, 1761.
(12) Shin, Y.-g. K.; Miskowski, V. M.; Nocera, D. G. *Inorg. Chem.* **1990**, *29*, 2308.

0020-1669/92/1331-2184$03.00/0

and suggest that some alternative assignments are necessary.

Experimental Section

Preparation of Compounds. The preparation of the compounds used in this investigation followed literature methods but with some modifications. Starting materials were synthesized Pt(II) complexes or of reagent grade.

$(NH_4)_2[Pt_2(SO_4)_4(H_2O)_2]\cdot H_2O$.[13] A sample of $Pt(NO_2)_2(NH_3)_2$[14] (0.312 g, 0.97 mmol) was added to 9 M H_2SO_4 (3 mL) and heated slowly with stirring to 118 °C in an oil bath. The reaction mixture began to darken in color between 60 and 80 °C, and brown NO_2 gas was evolved at 110 °C. The reaction progress was monitored by observing the NO_2 evolution, which ceased after ~2 h. H_2O (1 mL) was added when the reaction mixture had cooled to 60 °C; further cooling to ice temperature produced a yellow solid, which was collected by vacuum filtration and washed with ice-cold water, ethanol, and finally dry ether. The product was dried in vacuo overnight. The yield was low (16%), but the product gave satisfactory elemental analysis. The preparation was also carried out under a nitrogen atmosphere, but there was no increase in yield. The yield was increased slightly by using a slightly higher temperature (122 °C) for the reaction, but some grayish materials contaminated the product and necessitated recrystallization from hot water. All of the analyzed samples had the same UV–visible absorption spectrum.

$K_2[Pt_2(SO_4)_4(H_2O)_2]$.[13,15] Solid $K_2[Pt(NO_2)_4]\cdot 2H_2O$[14] (0.263 g, 0.53 mmol) was added to 9 M H_2SO_4 (2 mL) and heated slowly with stirring to 120 °C in an oil bath. The reaction mixture began to darken at room temperature and was followed by the evolution of NO_2 gas at 120 °C, which ceased after ~40 min. Upon cooling to 65 °C, 0.7 mL of H_2O was added, and the mixture was further cooled to ice temperature. The yellow product precipitated and was collected with dry ether. The product, which was dried in vacuo overnight, had a yield of 52%. The solution absorption spectrum was identical to that of the ammonium salt.

$(NH_4)_2[Pt_2(HPO_4)_4(H_2O)_2]$.[7,12,16] Solid $Pt(NO_2)_2(NH_3)_2$[14] (0.273 g, 0.32 mmol) was treated with 85% H_3PO_4 (2 mL). The mixture was heated slowly with stirring to 110 °C. Brown NO_2 gas evolution began at 80 °C and continued until the mixture had been stirred for ~1 h at 110 °C. After being cooled to ice temperature the dark red-brown solution was filtered and treated with solid $(NH_4)_2HPO_4$ (0.171 g, 2.3 mmol), which dissolved completely. H_2O (10 mL) was added, whereupon an immediate precipitation of a yellow solid took place. The solid was collected and washed with ice water, ethanol, and dry ether. After drying in vacuo overnight, the yield was 37% and the compound gave satisfactory elemental analysis. Attempts were made to prepare $Na_2[Pt_2(HPO_4)_4(H_2O)_2]$ from $Pt(NO_2)_2(NH_3)_2$ following the literature procedure,[7] but the product always contained nitrogen by elemental analysis, which suggests that a mixture of Na^+ and NH_4^+ salts were formed rather than the pure Na^+ salt.

$[(n\text{-}C_4H_9)_4N]_2[Pt_2(HSO_4)_2(SO_4)_2Cl_2]\cdot H_2O$. A small quantity (23.8 mg) of $(NH_4)_2[Pt_2(SO_4)_4(H_2O)_2]\cdot H_2O$ was dissolved in 9 M H_2SO_4 (5 mL) and treated with 4 M HCl (5 mL); the mixture was stirred until a clear yellow solution was formed. Excess $(n\text{-}C_4H_9)_4NCl$ was then added as a saturated aqueous solution, whereupon precipitation of product occurred. The mixture was cooled to ice temperature and the solid precipitate collected by filtration, washed with a minimal amount of ice-cold water (the product has a high solubility in water), ethanol, and finally dry ether. The yield was 48%, and the dried product gave satisfactory elemental analysis. Attempts were made to use an analogous procedure to prepare $[(n\text{-}C_4H_9)_4N]_4[Pt_2(HPO_4)_4Cl_2]$ from $(NH_4)_2[Pt_2(HPO_4)_4(H_2O)_2]$, but products analyzed as $[(n\text{-}C_4H_9)_4]_{4-x}[Pt_2(H_2PO_4)_x(HPO_4)_{4-x}Cl_2]$, $2 < x < 3$.

Solution Preparation of $Pt_2(B\text{-}B)_4X_2^{n-}$ Ions. The $Pt_2(B\text{-}B)_4X_2^{n-}$ ions, where B-B = HPO_4^{2-}, X = Cl^-, Br^-, and SMe_2 or B-B = SO_4^{2-}, X = Cl^-, Br^-, OH^-, and NH_3, were prepared in aqueous solution by axial water replacement reactions in the respective diaqua complexes.[7,12,17] In order to ensure complete replacement and to determine conditions where the product complexes were stable enough for spectral measurements, an extensive spectrophotometric study of the reactions was carried out. Each of the complexes has characteristic intense UV bands which allow the identification of the Pt species present and the determination of its stability with time. The spectra of the starting diaqua ions were found to be unchanged in acidic solution over times up to several days. Also there was no difference in the spectra of $(NH_4)_2[Pt_2(HPO_4)_4(H_2O)_2]$ in neutral aqueous solution and in 1 M $HClO_4$. However, $Pt_2(SO_4)_4(H_2O)_2^{2-}$ showed distinct changes in neutral solution compared to 2 M H_2SO_4. These changes are consistent with the hydrolysis in eq 1. At pH = 11.5

$$Pt_2(SO_4)_4(H_2O)_2^{2-} \rightleftharpoons Pt_2(SO_4)_4(H_2O)(OH)^{3-} + H^+ \quad (1)$$

the hydrolysis of both H_2O ligands was complete to form the $Pt_2(SO_4)_4(OH)_2^{4-}$ ion. The spectrum of the diaqua complex was restored when the dihydroxo complex was treated with acid ($HClO_4$) to give a solution of pH = 1–2.

The axial water ligands of the diaqua complexes are reversibly replaced by X in two equilibrium steps,[7,17] eqs 2 and 3. To ensure complete

$$Pt_2(B\text{-}B)_4(H_2O)_2^{2-} + X \underset{}{\overset{K_1}{\rightleftharpoons}} Pt_2(B\text{-}B)_4X(H_2O)^{n-} + H_2O \quad (2)$$

$$Pt_2(B\text{-}B)_4X(H_2O)_2^{2-} + X \underset{}{\overset{K_2}{\rightleftharpoons}} Pt_2(B\text{-}B)_4X_2^{n-} + H_2O \quad (3)$$

formation of the disubstituted complex, a sufficient excess of the ligand was added until the characteristic band(s) of $Pt_2(B\text{-}B)_4X_2^{n-}$ was (were) unchanged upon further addition of X. Under these conditions, the bands due to $Pt_2(B\text{-}B)_4X(H_2O)^{m-}$ and $Pt_2(B\text{-}B)_4(H_2O)_2^{2-}$ were absent. The $Pt_2(SO_4)_4(NH_3)_2^{2-}$ complex was formed by dissolving $K_2[Pt_2(SO_4)_4(H_2O)_2]$ in $NH_3/(NH_4)_2SO_4$ (0.59 M/0.225 M, pH = 9) buffer. The equilibrium for the formation of $Pt_2(HPO_4)_4(Me_2S)_2^{2-}$ was found to be far to the right; the overall (K_1K_2) equilibrium constant was estimated to be $\sim 10^7$ M^{-1}. The formation of the dihalo complexes was less favorable and required greater concentrations of excess Cl^- or Br^-. The reported values of K_1K_2 for the HPO_4^{2-} complexes are 209 and 462 M^{-1} for X = Cl^- and Br^-, respectively.[7] The $Pt_2(SO_4)_4Br_2^{4-}$ and $Pt_2(HPO_4)_4Br_2^{4-}$ complexes in the presence of excess Br^- were also found to be unstable with respect to a photocatalyzed reaction that forms $PtBr_6^{2-}$. The absorption spectrum was observed to change with time almost immediately upon formation of the dibromo complexes. Care was taken to minimize the extent of this reaction when spectral data were collected; the HPO_4^{2-} complex reacted more slowly than the SO_4^{2-} complex. Solutions were prepared in the dark and spectra were measured immediately. Even so, reliable MCD data could only be obtained for $Pt_2(HPO_4)_4Br_2^{2-}$ because of the time required for the scans (typically 0.5 h). The spectra for the dichloro complexes were unchanged during the time required for measurements, and no evidence for an analogous decomposition was observed. Also, the absorption spectrum of $[(n\text{-}C_4H_9)_4N]_2[Pt_2(HSO_4)_4Cl_2]\cdot H_2O$ dissolved in 2 M HCl was identical to the spectrum of the dichloro complex produced by treating the $Pt_2(SO_4)_4(H_2O)_2^{2-}$ salts with 2 M HCl.

Spectral Measurements. Absorption spectra were measured by means of a Cary 1501 or Cary 17D spectrophotometer. Absorption and MCD spectra were determined simultaneously and synchronously along the same light path by means of a spectrometer described earlier.[18] The field was provided by a 7-T superconducting magnet (Oxford Instruments SM2-7, equipped with a room-temperature bore tube). All spectra were corrected for solvent and any excess ligand in a blank. Beer's law was found to hold within experimental error when the X:Pt ratio was maintained.

A low-temperature (77 K) measurement was made for a poly(vinyl alcohol) (PVA) film containing $(NH_4)_2[Pt_2(HPO_4)_4(H_2O)_2]$. The film was prepared by dissolving 194 mg of PVA in 3 mL of hot H_2O containing 2 drops of 1 M $HClO_4$ and 8 mg of the complex. The solution was spread on microscope slides and allowed to dry for 24 h. It was then carefully pealed off the slides and suspended in liquid nitrogen in a cryostat situated in the light beam of the spectrophotometer. There was no apparent reduction in the intensity at low temperature of the band at 2.54 μm^{-1}, consistent with the presence of an allowed transition. This result is similar to the low-temperature absorption measurement for $Pt_2(HPO_4)_4Cl_2^{4-}$ in a LiCl/HCl glass at 77 K reported recently.[12]

Results and Discussion

Electronic Absorption and MCD Spectra. The electronic absorption and 7.0-T MCD spectra for aqueous solutions of $Pt_2(B\text{-}B)_4(H_2O)_2^{2-}$, $Pt_2(B\text{-}B)_4Cl_2^{4-}$, B-B = SO_4^{2-} and HPO_4^{2-}; $Pt_2(HPO_4)_4X_2^{n-}$, X = Br^- and Me_2S; and $Pt_2(SO_4)_4X_2^{n-}$, X = NH_3 and OH^- are presented in Figures 1–4, respectively. Quantitative

(13) Muraveiskaya, G. S.; Kukina, G. A.; Orlova, V. S.; Evstaf'eva, O. N.; Porai-Koshits, M. A. *Dokl. Akad. Nauk. SSSR* **1976**, *226*, 76.
(14) Grube, H. L. *Handbook of Preparative Inorganic Chemistry*; Brauer, G., Ed.; Academic Press: New York, 1965; Vol. 2, p 1579.
(15) Orlova, V. S.; Muraveiskaya, G. S.; Evstaf'eva, O. N. *Russ. J. Inorg. Chem. (Engl. Transl.)* **1975**, *20*, 753.
(16) Muraveiskaya, G. S.; Abashkin, V. E.; Evstaf'eva, O. N.; Golovaneva, I. F.; Shchelokov, R. N. *Sov. J. Coord. Chem. (Engl. Transl.)* **1981**, *6*, 218.
(17) El-Mehdawi, R.; Fronczek, F. R.; Roundhill, D. M. *Inorg. Chem.* **1986**, *25*, 1155.
(18) Mason, W. R. *Anal. Chem.* **1982**, *54*, 646.

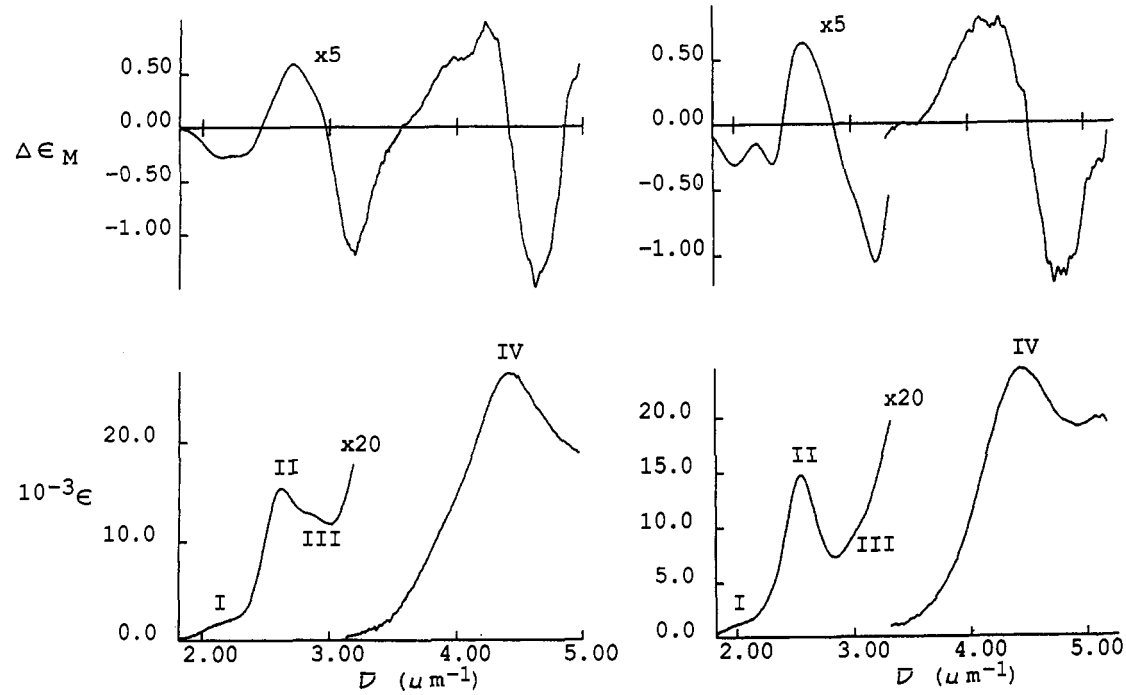

Figure 1. Electronic absorption (lower curves) and MCD (upper curves) spectra for $(NH_4)_2[Pt_2(SO_4)_4(H_2O)_2]\cdot H_2O$ in 0.10 M H_2SO_4 (left) and for $(NH_4)_2[Pt_2(HPO_4)_4(H_2O)_2]$ in 0.10 M $HClO_4$ (right). The units for ϵ and $\Delta\epsilon_M$ are M^{-1} cm^{-1} and M^{-1} cm^{-1} T^{-1}, respectively.

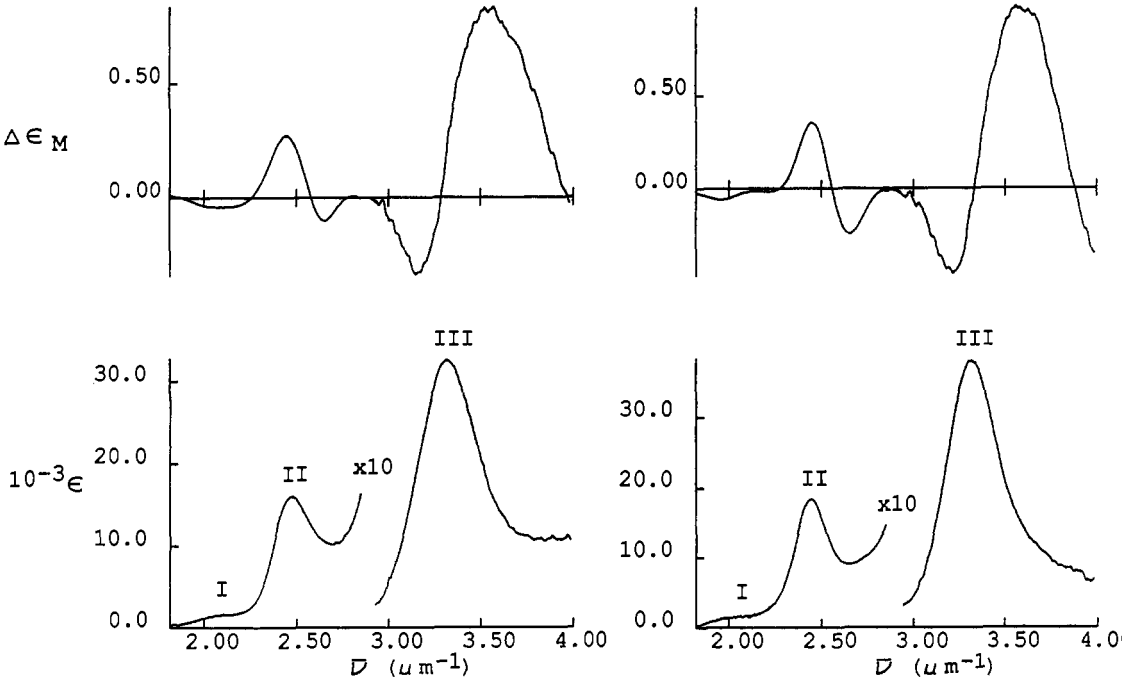

Figure 2. Electronic absorption (lower curves) and MCD (upper curves) spectra for $[Pt_2(SO_4)_4Cl_2]^{4-}$ in 2.0 M HCl and 0.05 M H_2SO_4 (left) and for $[Pt_2(HPO_4)_4Cl_2]^{4-}$ in 2.0 M HCl and 0.05 M $HClO_4$ (right). Units as in Figure 1.

spectral data for these complexes are collected in Table I.[19] Apart from minor differences, Figures 1 and 2 show that the absorption and MCD for the diaqua and dichloro complexes are nearly the same for the SO_4^{2-} and HPO_4^{2-} bridging ligands. The similarity demonstrates that the energy levels and excited states for the $Pt_2O_8^{2-}$ skeletal structure are not much affected by changing the oxo-bridging ligands from SO_4^{2-} to HPO_4^{2-}. The general shape of the absorption spectra in Figures 1–4 is similar and consists of several lower energy bands with $\epsilon = \sim 3000$ M^{-1} cm^{-1} or less and one or more higher energy bands that are more intense with $\epsilon > 20000$ M^{-1} cm^{-1}. This pattern is quite similar to that observed for a number of $Pt_2(POP)_4X_2^{n-}$ complexes, which has prompted the analogous assignment proposal noted earlier.[12] In contrast to the absorption spectra, the shape of the MCD spectra in Figures 1–4 depends upon the nature of the X ligand, and differing patterns of positive or negative *A* and *B* terms[20] are observed in various

(19) The molar absorptivity determined for band IV for $(NH_4)_2[Pt_2(HPO_4)_4(H_2O)_2]$ in 0.10 M $HClO_4$ (ϵ = 24 300 M^{-1} cm^{-1}) differs significantly from the value reported for $Na_2[Pt_2(HPO_4)_4(H_2O)_2]$ in water (ϵ = 16 160 M^{-1} cm^{-1})[7,17] and for $K_2[Pt_2(HPO_4)_4(H_2O)_2]$ in water (ϵ not given numerically but estimated to be ~16 600 M^{-1} cm^{-1} from Figure 1[12]). The origin of the difference is not known, but the value given in Table I was determined from several independent measurements with different analyzed samples, all in dilute acid (0.10 M $HClO_4$) to prevent hydrolysis. Furthermore, the absorptivity for band IV for $(NH_4)_2[Pt_2(SO_4)_4(H_2O)_2]\cdot H_2O$ in 0.10 M H_2SO_4 (ϵ = 27 400 M^{-1} cm^{-1}), measured from analyzed samples and under comparable conditions, has a value closer to the value for the HPO_4^{2-} complex found here than to the literature values.

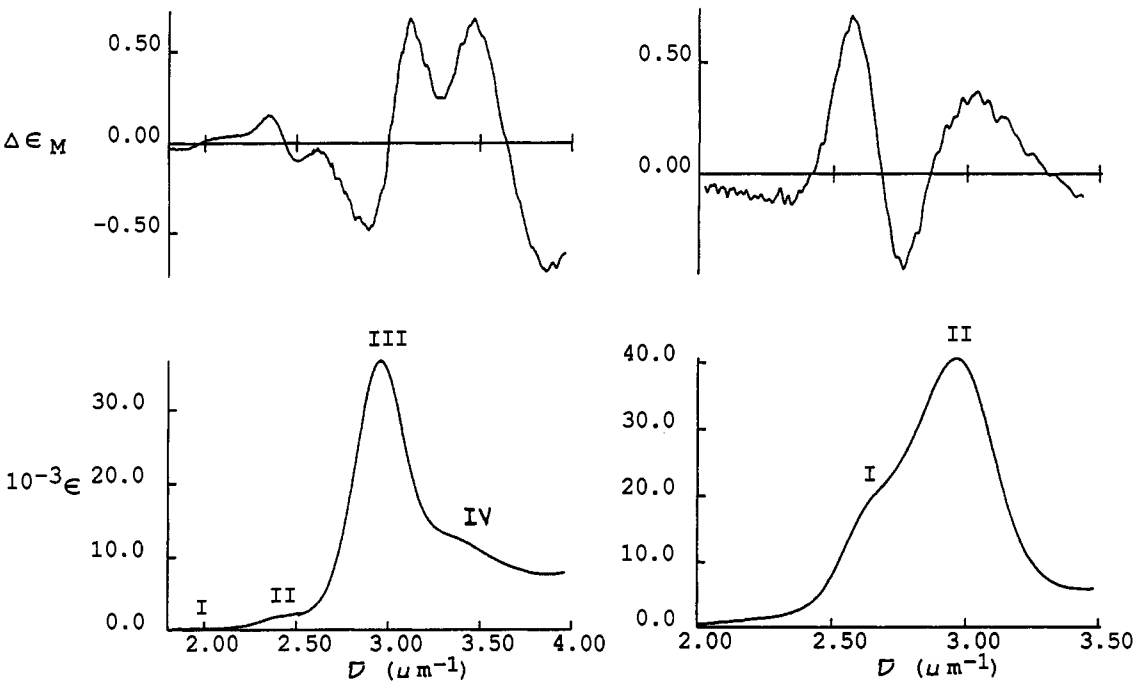

Figure 3. Electronic absorption (lower curves) and MCD (upper curves) spectra for $[Pt_2(HPO_4)_4Br_2]^{4-}$ in 1.9 M NH_4Br and 0.05 M $HClO_4$ (left) and for $[Pt_2(HPO_4)_4(Me_2S)_2]^{2-}$ in 1.56×10^{-2} M Me_2S (right). Units as in Figure 1.

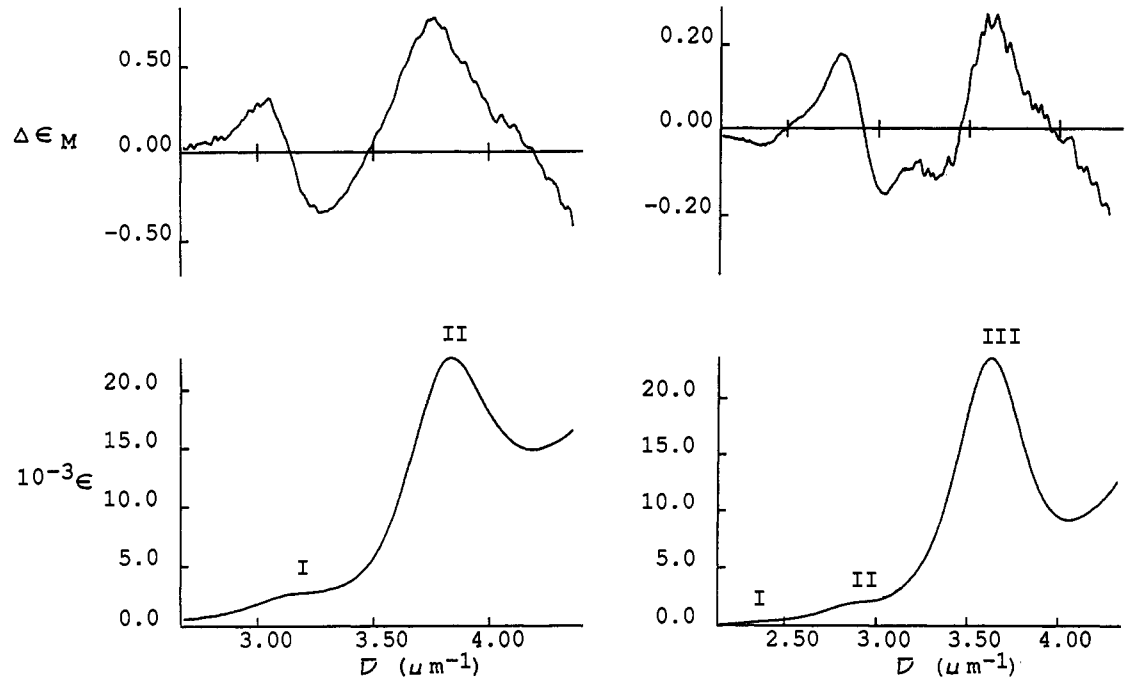

Figure 4. Electronic absorption (lower curves) and MCD (upper curves) spectra for $[Pt_2(SO_4)_4(NH_3)_2]^{2-}$ in 0.225 M $(NH_4)_2SO_4$ and 0.590 M NH_3 (left) and for $[Pt_2(SO_4)_4(OH)_2]^{4-}$ in 8.75×10^{-3} M NaOH (right). Units as in Figure 1.

combinations for the different complexes. Furthermore, the MCD spectra for $Pt_2(HPO_4)_4X_2^{4-}$, X = Cl^- (Figure 2) and Br^- (Figure 3), are substantially different from the MCD spectra reported[11] for $Pt_2(POP)_4X_2^{4-}$, X = Cl^- and Br^-, even though there are similarities in the absorption spectra for the analogous HPO_4^{2-} and POP complexes. Thus the MCD spectra indicate that the spectral assignments given for the POP complexes cannot be applied in any simple way to the HPO_4^{2-} or SO_4^{2-} complexes and that detailed assignments must reflect the X ligand dependence.

(20) For a review of MCD spectroscopy together with the standard (Stephens) conventions adopted here, see: Piepho, S. B.; Schatz, P. N. *Group Theory in Spectroscopy with Applications to Magnetic Circular Dichroism*; Wiley-Interscience: New York, 1983.

Molecular Orbitals, Electronic Excited States, and MCD Terms. In order to interpret the absorption and MCD spectra, a MO energy level scheme was developed with the assumption of D_{4h} symmetry for the XPt_2O_8X skeletal structure. This scheme is presented in Figure 5; the z axis is taken along X–Pt–Pt–X and the coordinate system is right-handed as shown in **1**. The ground-state electron configuration is $...(2e_u)^4(b_{1u})^2(b_{2g})^2(2e_g)^4$ and is thus diamagnetic, totally symmetric, and designated $^1A_{1g}$. The highest energy occupied MO (HOMO) is not known for certain, but it is likely either $2e_g$ ($d\pi^*$) or the b_{1u}, b_{2g} ($d\delta$,$d\delta^*$) pair. The lowest energy unoccupied orbitals are expected to be $2a_{2u}$ ($d\sigma^*$) and the b_{1g}, b_{2u} σ^*PtO_4 pair. These latter orbitals are mainly Pt-based $d_{x^2-y^2}$ orbitals which are Pt–O antibonding. Table II lists the probable low-energy excited configurations for the

Table I. Spectral Data

band no.	absorption $\bar{\nu}$, μm^{-1}	absorption λ, nm	absorption ϵ, M^{-1} cm^{-1}	MCD $\bar{\nu}$, μm^{-1}	MCD $\Delta\epsilon_M$, (M cm T)$^{-1}$	excited state[c]
			$(NH_4)_2[Pt_2(SO_4)_4(H_2O)_2]\cdot H_2O$ in 0.10 M H_2SO_4			
I	2.15	466	89[a]	2.15	−0.055[a]	$1E_u$, $1A_{2u}$
II	2.62	381	790	2.27[b]	−0.053	$2E_u$
				2.46[b]	0	
				2.73[b]	+0.121	
III	2.74	347	650			(B_{1u})
				3.19	−0.242	$10A_{2u}$, $11A_{2u}$?
				4.00	+0.60[a]	
IV	4.43	226	27400	4.23[b]	+0.99	$19E_u$, $21E_u$
				4.41[b]	0	
				4.63[b]	−1.52	
			$(NH_4)_2[Pt_2(HPO_4)_4(H_2O)_2]$ in 0.10 M $HClO_4$			
I	2.01	498	65	2.01	−0.061	$1E_u$, $2A_{2u}$
II	2.55	393	740	2.33[b]	−0.060	$2E_u$
				2.42[b]	0	
				2.58[b]	+0.126	
III	3.01	333	474[a]			(B_{1u})
				3.20	−0.211	$10A_{2u}$, $11A_{2u}$?
IV	4.45	225	24300	4.18[b]	+0.77	$19E_u$, $21E_u$
				4.52[b]	0	
				4.77[b]	−1.11	
			$[Pt_2(SO_4)_4Cl_2]^{4-}$ in 2.0 M HCl and 0.05 M H_2SO_4			
I	2.09	478	200[a]	2.09	−0.038	$1E_u$, $1A_{2u}$
II	2.47	404	1980	2.44	+0.270	$2E_u$, (B_{1u})
				2.66	−0.097	$4E_u$?
III	3.32	301	34300	3.15[b]	−0.30	$10E_u$
				3.29[b]	0	
				3.54[b]	+0.80	
			$[Pt_2(HPO_4)_4Cl_2]^{4-}$ in 2.0 M HCl and 0.05 M $HClO_4$			
I	2.00	500	155[a]	1.95	−0.058	$1E_u$, $1A_{2u}$
				2.20	−0.020[a]	
II	2.45	409	2000	2.45	+0.349	$2E_u$, (B_{1u})
				2.65	−0.238	$4E_u$?
				3.21	−0.46	
III	3.31	302	40000	3.33[b]	0	$10E_u$
				3.59	+0.93	
			$[Pt_2(SO_4)_4Br_2]^{4-}$ in 2.0 M NH_4Br and 1.0 M H_2SO_4			
II	2.35	426	2350[a]			$2E_u$, (B_{1u})
III	2.87	348	40400			$10E_u$
IV	3.25	308	14800[a]			$12E_u$
			$[Pt_2(HPO_4)_4Br_2]^{4-}$ in 1.9 M NH_4Br and 0.05 M $HClO_4$			
I	1.93	517	205[a]	1.86	−0.030	$1E_u$, $1A_{2u}$
				2.08	+0.034[a]	
II	2.44	410	2000[a]	2.35	+0.15	$2E_u$, (B_{1u})
				2.50	−0.099	$4E_u$?
III	2.95	339	41000	2.88[b]	−0.43	$10E_u$
				3.00[b]	0	
				3.11[b]	+0.66	
IV	3.35	299	12900[a]	3.46[b]	+0.66	$12E_u$
				3.65[b]	0	
				3.86[b]	−0.69	
			$[Pt_2(HPO_4)_4(Me_2S)_2]^{2-}$ in 1.56×10^{-2} M Me_2S			
				2.30	−0.15	$11E_u$, $6A_{2u}$
I	2.66	376	20100[a]	2.57[b]	+0.74	$12E_u$
				2.68[b]	0	
				2.75[b]	−0.38	
II	2.96	338	41000	3.04	+0.40	$[8A_{2u} + 4A_{2u}]$
			$[Pt_2(SO_4)_4(NH_3)_2]^{2-}$ in 0.225 M $(NH_4)_2SO_4$ and 0.590 M NH_3			
I	3.14	318	2600[a]	3.03[b]	+0.30	$4E_u$?
				3.13[b]	0	
				3.26[b]	−0.33	
II	3.84	261	23000	3.77	+0.84	$[8A_{2u} + 4A_{2u}]$
			$[Pt_2(SO_4)_4(OH)_2]^{4-}$ in 8.75×10^{-3} M NaOH			
I	2.35	426	490[a]	2.35	−0.041	$3E_u$, $2A_{2u}$
II	2.88	347	2400	2.79[b]	+0.178	$4E_u$?
				2.92[b]	0	
				3.03[b]	−0.148	
				3.31	−0.124[a]	$8E_u$?
III	3.62	276	25000	3.62	+0.24	$[8A_{2u} + 4A_{2u}]$

[a] Shoulder. [b] MCD *A* term. [c] Refer to Table II.

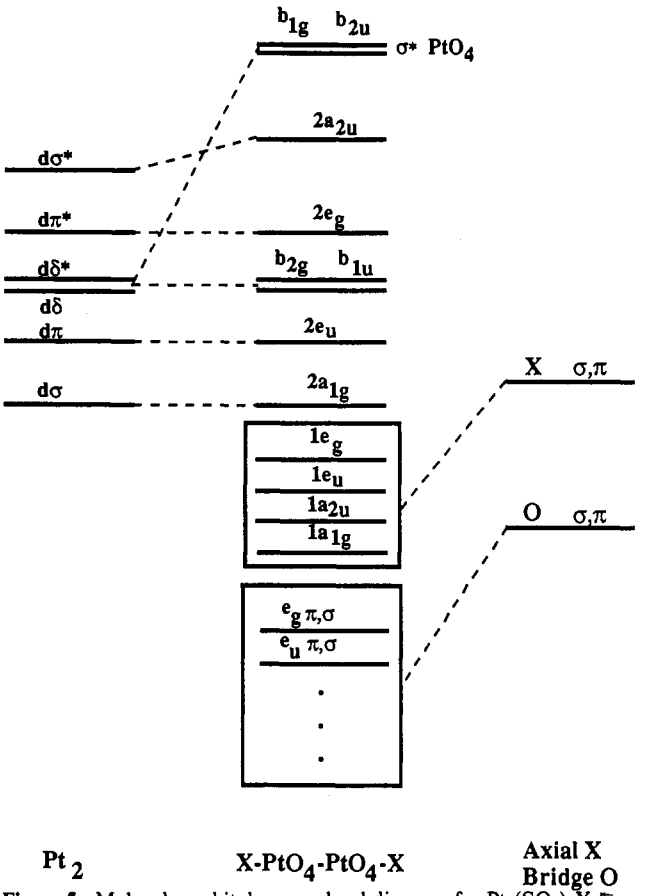

Figure 5. Molecular orbital energy level diagram for $Pt_2(SO_4)_4X_2^{n-}$ or $Pt_2(HPO_4)_4X_2^{n-}$ ions assuming D_{4h} symmetry. The z axis is along X–Pt–Pt–X.

$Pt_2(B\text{-}B)_4X_2^{n-}$ complexes. The singlet and triplet excited states from these configurations are visualized as suitable "zero-order" states for interpreting the spectra. However, these states neglect the influence of Pt spin–orbit coupling, which is known to be important for orbitals constructed from 5d atomic orbitals ($\zeta_{5d} \sim 3000$ cm^{-1} for Pt). The main influence of spin–orbit coupling is to intermix the singlet and triplet states, which will allow transitions to formally spin-forbidden triplet states to gain intensity. The spin-orbit states for each singlet and triplet zero-order excited state are given in Table II also; they are characterized by the absence of spin multiplicity superscripts. In D_{4h} symmetry electric dipole allowed transitions are limited to A_{2u} (z-polarized) and E_u (x,y-polarized) states. Transitions to A_{1u}, B_{1u}, or B_{2u} are symmetry forbidden, are expected to be 1 order of magnitude weaker, and are therefore obscured by the more intense allowed transitions.

Transitions to either A_{2u} or E_u states can exhibit MCD B terms, which originate from magnetic mixing of the A_{2u} state or the E_u state with other E_u states in the presence of the magnetic field. Only transitions to the degenerate E_u states, however, can exhibit MCD A terms because they arise from a Zeeman splitting of the degenerate state by the field. The sign of the A terms for transitions to the E_u states can be determined from the $\bar{A}_1/\bar{D}_0$ parameter ratio in a standard way[20] for nonisotropic molecules in solution from eq 4, where $\bar{D}_0 = {}^1/_3|\langle A_{1g}||\mathbf{m}||E_u(i)\rangle|^2$ and is related

$$\bar{A}_1/\bar{D}_0 = \frac{-1}{2^{1/2}\mu_B}\langle (E_u(i)||\mathbf{u}||E_u(i)\rangle \qquad (4)$$

to the electric dipole strength of the transition, μ_B is the Bohr magnetron, and $\mathbf{u} = -\mu_B(\mathbf{L} + 2\mathbf{S})$ and $\mathbf{m} = e\mathbf{r}$, the magnetic and electric moment operators. By approximating the one-electron MOs as 5d atomic orbitals on Pt or np atomic orbitals on X or O and adopting a one-center approximation to the reduced matrix element in eq 4, the sign of the $\bar{A}_1/\bar{D}_0$ ratio can be determined.[20] This quantity is also included in Table II to help guide the interpretation of the MCD spectra. It should be remarked here that,

Table II. Excited Configurations and States

excited confgn[a]	excited states (no spin–orbit coupling)	spin–orbit states[b]	$\bar{A}_1/\bar{D}_0$ sign[c]
$(2e_g)^3(2a_{2u})$	^3E_u	$1E_u$, $1A_{2u}$	+
	^1E_u	$2E_u$	+
$(2e_g)^3(b_{2u})$	^3E_u	$3E_u$, $2A_{2u}$	−
	^1E_u	$4E_u$	−
$(b_{2g})(2a_{2u})$	$^3B_{1u}$	$5E_u$	+
$(2e_u)^3(b_{1g})$	^3E_u	$6E_u$, $3A_{2u}$	−
	^1E_u	$7E_u$	−
$(2a_{1g})(2a_{2u})$	$^3A_{2u}$	$8E_u$	+
	$^1A_{2u}$	$4A_{2u}$	
$(1e_g)^3(2a_{2u})$	^3E_u	$9E_u$, $5A_{2u}$	+
	^1E_u	$10E_u$	+
$(1e_g)^3(b_{2u})$	^3E_u	$11E_u$, $6A_{2u}$	−
	^1E_u	$12E_u$	−
$(1e_u)^3(b_{1g})$	^3E_u	$13E_u$, $7A_{2u}$	−
	^1E_u	$14E_u$	−
$(1a_{1g})(2a_{2u})$	$^3A_{2u}$	$15E_u$	+
	$^1A_{2u}$	$8A_{2u}$	
$(e_g\pi,\sigma)^3(2a_{2u})$	^3E_u	$16E_u$, $9A_{2u}$	+[d]
	^1E_u	$17E_u$	+[d]
$(e_g\pi,\sigma)^3(b_{2u})$	^3E_u	$18E_u$, $10A_{2u}$	−[d]
	^1E_u	$19E_u$	−[d]
$(e_u\pi,\sigma)^3(b_{1g})$	^3E_u	$20E_u$, $11A_{2u}$	−[d]
	^1E_u	$21E_u$	−[d]

[a] Filled orbitals omitted. Ground-state configuration ... $(b_{1u})^2(b_{2g})^2(2e_g)^4$, $^1A_{1g}$. [b] Symmetry-forbidden A_{1u}, B_{1u}, and B_{2u} states from ^3E_u states, B_{2u} state from $^3B_{1u}$ state, and A_{1u} states from $^3A_{2u}$ states are omitted. [c] Determined for the E_u states from eq 4. [d] σ, π mixing required in a one-centered approximation.[21]

because of the approximations involved, *quantitative* magnitudes for the $\bar{A}_1/\bar{D}_0$ ratios cannot be given with confidence. However, the use of eq 4 to predict the sign, and thus the shape, of the MCD A term is considered reliable. The signs of the MCD B terms are more problematic because they will be determined from a summation of terms, weighted inversely by energy differences for the interaction of a given A_{2u} or E_u state with all other E_u states. They are therefore highly dependent upon the magnitude of the interaction and the specific level structure of the system. The presence of B terms for E_u states will serve to make observed A terms unsymmetrical or could obscure the A term completely if they were very large in comparison to the A terms. Finally, MCD C terms, of course, will be absent because the ground state is diamagnetic.

Spectral Interpretation. Even though a common spectral interpretation is expected to apply to the SO_4^{2-} and HPO_4^{2-} complexes with the same axial ligand X, the marked dependence of the MCD spectra on the nature of X, especially for the most intense bands, argues convincingly for different band assignments for the different types of X ligand. Therefore, a separate interpretation of the absorption and MCD spectra for the complexes of each type of X ligand is presented in the following sections. The proposed band assignments which result are summarized in Table I; the excited states listed there refer to the spin–orbit states given in Table II.

$Pt_2(SO_4)_4(H_2O)_2^{2-}$ and $Pt_2(HPO_4)_4(H_2O)_2^{2-}$. The high-energy intense band in the absorption spectra of the diaqua complexes (band IV, Figure 1) is broad and accompanied by a negative A term in the MCD spectra. The intensity of this band is clearly consistent with an allowed transition to a state of predominantly singlet origin, but the presence of the A term implies a transition to a degenerate E_u excited state. Thus, the previous assignment[7,12] of this band as a spin-allowed $d\sigma \rightarrow d\sigma^*$ transition cannot be correct because this excitation would necessarily give a nondegenerate A_{2u} excited state. The negative sign for the A term narrows the choice of the E_u excited state for an acceptable band assignment (see Table II). However, a ligand to metal charge transfer (LMCT) involving the axial H_2O ligands, $1e_g \rightarrow b_{2u}$ or $1e_u \rightarrow b_{1g}$, is unlikely because of the stability of the filled H_2O orbitals. The remaining possibilities include transitions to $4E_u$ ($2e_g \rightarrow b_{2u}$, $d\pi^* \rightarrow \sigma^*PtO_4$), $7E_u$ ($2e_u \rightarrow b_{1g}$, $d\pi \rightarrow \sigma^*PtO_4$), $19E_u$ ($e_g\pi,\sigma \rightarrow b_{2u}$, bridge O $\rightarrow$ Pt LMCT), and $21E_u$ ($e_u\pi,\sigma \rightarrow b_{1g}$,

bridge O → Pt LMCT). The energy and the intensity of the transitions to $4E_u$ and $7E_u$ (which are analogous to ligand field transitions in a mononuclear complex) are expected to be lower than for the LMCT transitions to $19E_u$ or $21E_u$, which makes these latter two logical choices. It must be noted that the σ and π e_g and e_u orbitals on the bridge oxygens must be mixed in order for the MCD *A* terms to be nonzero in a one-centered approximation. The σ, π mixing has been described in detail for square AuX_4^- complexes,[21] and this mixing can be applied in an entirely analogous way to the square PtO_4 units of the binuclear complexes here. Band IV for the diaqua complexes is quite broad (fwhm ~ 0.8–1.0 μm^{-1}), and it is easy to visualize more than one transition beneath its envelope. If the $19E_u$ and $21E_u$ states are not widely separated in energy as might be reasonably expected, say less than 5000 cm^{-1}, and if their transition bandwidths are typical (~2000–4000 cm^{-1}), then band IV could encompass both the transitions to $19E_u$ and $21E_u$. It is easy to show that the MCD for such a situation will be a simple superposition of the negative *A* terms because the magnetic mixing between $19E_u$ and $21E_u$ will be very small due to orbital orthogonality, and hence *B* terms from such an interaction will be negligible. The interpretation of band IV as containing transitions to both $19E_u$ and $21E_u$, though somewhat speculative, would provide an explanation for the bandwidth, together with the negative *A* term shape of the MCD spectra.

In contrast to band IV, bands I–III are much weaker and are less broad. Band II in each case is the most prominent. The 77 K absorption measurement for $(NH_4)_2[Pt_2(HPO_4)_4(H_2O)_2]$ in a PVA film (see Experimental Section) showed that the intensity of band II does not decrease on cooling, which implies a fully allowed transition. The MCD for band II shows an unsymmetrical positive *A* term, which indicates the presence of an E_u state. In view of its energy, the logical assignment of band II is to the transition to $2E_u$ ($2e_g \rightarrow 2a_{2u}$), the $d\pi^* \rightarrow d\sigma^*$ excitation. The assignment of band I to the unresolved transitions to $1E_u$ and $1A_{2u}$ spin–orbit states of ^3E_u $(2e_g)^3(2a_{2u})$ then follows. These states will certainly give rise to strong *B* term interactions with $2E_u$ in the presence of the field, which can thus account for the unsymmetrical *A* term for the latter. The *A* term for $1E_u$ is also likely obscured by the strong *B* terms for these weak unresolved transitions. The assignment of band I is also consistent with the recent luminescence studies[12] for $Pt_2(HPO_4)_4(H_2O)_2^{2-}$, which ascribed the observed emission to the spin–orbit states of ^3E_u $(2e_g)^3(2a_{2u})$ at lowest energy. Finally, band III, which is poorly resolved, especially for the HPO_4^{2-} complex, has been assigned[12] as the $d\delta^* \rightarrow d\sigma^*$ excitation $b_{2g} \rightarrow 2a_{2u}$. The transition to the B_{1u} excited state is dipole forbidden in D_{4h} symmetry and therefore should be weak, which would account for the poor resolution of band III. The MCD spectra offer little assistance in the interpretation of band III since no well-defined terms are observed. There is, however, a prominent negative MCD minimum near 3.2 μm^{-1} which is not due to band III. The transition responsible for this MCD feature is not resolved in the absorption spectra. The minimum gives the appearance of a *B* term and might signal the presence of an A_{2u} state higher in energy than band III but lower in energy than band IV. Certainly the $10A_{2u}$ and also the $11A_{2u}$ states are expected on the lower energy side of the intense band IV, but little more can be concluded from the present results.

$Pt_2(SO_4)_4X_2^{4-}$ and $Pt_2(HPO_4)_4X_2^{4-}$, X = Cl^- and Br^-. In contrast to the negative *A* term in the MCD for the intense high-energy band in the diaqua complexes, the intense counterpart in the dichloro complexes (band III, Figure 2) is characterized by a positive *A* term in the MCD spectra, although the *A* term is rather unsymmetrical, and the positive high-energy portion is very broad. The *A* term, again, is inconsistent with the previous assignments[7,12] of band III as $(X\sigma, d\sigma) \rightarrow d\sigma^*$ because the excited state for this assignment must be nondegenerate, as discussed above for the diaqua complexes. An assignment which would be consistent with the *A* term is the transition to the predominantly singlet $10E_u$ state, the $X\pi \rightarrow d\sigma^*$ LMCT excitation $1e_g \rightarrow 2a_{2u}$. Figure 3 (left-hand side) shows that band III and the corresponding positive *A* term for $Pt_2(HPO_4)_4Br_2^{4-}$ shifts ~3000 cm^{-1} to the red compared to $Pt_2(HPO_4)_4Cl_2^{4-}$ (Figure 2, right-hand side), as expected for a LMCT transition. The red shift of band III for the dibromo complex reveals the origin of the broadness in the high-energy part of the *A* term for the dichloro complex. A negative *A* term centered at 3.65 μm^{-1} and associated with the broad-shoulder band IV is observed for the dibromo complex, which undoubtedly is obscured by band III for the dichloro complex. The low-energy positive portion of this negative *A* term is assumed to overlap with the positive portion of this negative *A* term for band III and to give the very broad positive MCD on the high-energy side of band III shown in Figure 2. The broad-shoulder band IV and the negative *A* term for the dibromo complex is assigned to the LMCT transition to $13E_u$ ($1e_g \rightarrow b_{2u}$, $X\pi \rightarrow \sigma^*PtO_4$).

The lower energy weaker bands I and II for the dichloro and dibromo complexes have a pattern in the MCD spectra which is similar. The pattern also bears similarity to that observed for the low-energy bands of the diaqua complexes. Further, the band energies for the dihalo and diaqua complexes are not very different. These observations all suggest parallel $d\pi^* \rightarrow d\sigma^*$ assignments for the dihalo and diaqua complexes for bands I and II. The $d\pi^* \rightarrow d\sigma^*$ excitation is expected to be predominantly metal localized and therefore should not be strongly affected by changing the X ligand from water to a halide. The small shifts (0.1–0.2 μm^{-1}) between features in both the absorption and MCD spectra are consistent with this expectation. The same common assignments were also assumed for the $Pt_2(HPO_4)_4(H_2O)_2^{2-}$ and $Pt_2(HPO_4)_4X_2^{4-}$, X = Cl^- and Br^-, in the recent luminescence studies.[12] The characteristics of bands I and II contrast those of the higher energy intense bands, which because of their different origin red shift by 1.2–1.5 μm^{-1} from the diaqua to the dihalo complexes and exhibit entirely different MCD patterns.

Finally, the dihalo complexes exhibit a negative MCD minimum (near 2.65 μm^{-1} for the dichloro complexes and at 2.50 μm^{-1} for the dibromo complex) that does not correspond to any resolved absorption feature. These negative MCD signals seem to be analogous to the negative MCD band near 3.2 μm^{-1} observed for the diaqua complexes. The red shift of the dihalo minima compared to the diaqua complexes makes the MCD spectra in this region appear like negative *A* terms because of the positive signals associated with band II to lower energy. Interpretation of these negative MCD features is difficult without a resolved absorption band, but a negative *A* term, which implies the presence of an E_u state, slightly higher in energy than band II is certainly a possibility. The transition to $4E_u$ ($2e_g \rightarrow b_{2u}$, $d\pi \rightarrow \sigma^*PtO_4$) might be visualized in this energy region, but without more resolution this suggestion is admittedly speculative.

$Pt_2(HPO_4)_4(Me_2S)_2^{2-}$. The absorption spectrum for the Me_2S complex shows two intense bands in the 2.5–3.2-μm^{-1} region (Figure 3, right-hand side): a shoulder which is accompanied by a negative *A* term in the MCD spectrum and a maximum which has a corresponding *B* term. The low energy and high intensity of these bands compared to the onset of high-intensity bands in the diaqua complexes suggest a LMCT assignment. The higher energy orbitals of Me_2S compared to those of H_2O is consistent with the red shift observed in the spectra. Band I is therefore assigned as $S\pi \rightarrow \sigma^*PtO_4$, which gives rise to $12E_u$, consistent with the negative *A* term, and band II is assigned as $(S\sigma, d\sigma) \rightarrow d\sigma^*$, which would correspond to an A_{2u} state with contribution from the predominantly singlet $8A_{2u}$ and $4A_{2u}$ states. It should be clear that the Me_2S ligand must be visualized as a structureless "sulfide" ligand in order to preserve the approximate D_{4h} symmetry. The spectral detail is not sufficient to discuss departures from this first approximation to the interpretation.

$Pt_2(SO_4)_4(NH_3)_2^{2-}$ and $Pt_2(SO_4)_4(OH^-)_2^{4-}$. The spectra for the diammine and dihydroxo complexes (Figure 4) show intense bands at 3.84 (band II) and 3.62 μm^{-1} (band III), respectively, both of which have a positive *B* term associated with them in the MCD spectra. The *B* term is consistent with a transition to an A_{2u} state, and the logical assignment is to the axial LMCT ($X\sigma$,

(21) Isci, H.; Mason, W. R. *Inorg. Chem.* **1983**, *22*, 2266.

$d\sigma) \rightarrow d\sigma^*$ state, which is a combination of $4A_{2u}$ and $8A_{2u}$ of singlet origin. The $X\sigma$ donor orbitals are less stable than for H_2O, so that a lower energy axial LMCT is reasonable. The similarity in energy for the intense band for the diammine and dihydroxo complexes suggests that the axial ligands have σ orbitals of nearly the same stability in the two cases.

The lower energy bands for these complexes are not very well resolved and consist of shoulder absorption between 2.3 and 3.2 μm^{-1}. In both cases, the MCD has the appearance of a negative A term (for band I for the diammine complex and for band II for the dihydroxo complex). This MCD A term is ascribed to the transition to $4E_u$ ($2e_g \rightarrow b_{2u}$, $d\pi^* \rightarrow \sigma^*PtO_4$), which is expected to be the lowest energy negative A term of singlet parentage. This is the same state suggested at low energy in the dihalo complexes (and possibly also present among the low-energy bands for the diaqua complex). For the dihydroxo complex, an additional negative MCD feature is observed at 3.31 μm^{-1}, but no corresponding absorption is resolved. This MCD minimum signals the presence of another state between those associated with bands II and III. It is likely due to a transition to a state of spin-forbidden origin such as $8E_u$, but little more can be concluded from the present results. Finally, the weak band I for the dihydroxo complex is assigned as transitions to states of spin-forbidden origin $3E_u$ and $2A_{2u}$, which are expected to be at low energy.

Concluding Remarks. The energy level scheme in Figure 5 provides a basis for visualizing the excited configurations and states of Table II, which in turn provide a satisfactory interpretation of the spectra for the binuclear sulfato and hydrogen phosphatodiplatinum(III) complexes. Of course, other interpretations may be possible, but the assignments proposed here are internally consistent in energy, intensity, and MCD A term sign. One of the most important results to come from this study is the observation of A terms for the intense high-energy bands for the diaqua and dihalo complexes. These A terms demonstrate the presence of E_u states of LMCT origin rather than the A_{2u} $(X\sigma,d\sigma)d\sigma^*$ states assumed earlier.[7,12] Furthermore, a consideration of A term signs allows more detailed assignments of these intense bands. The diaqua complexes reveal LMCT involving the bridge oxygen ligands while the dihalo complexes give rise to LMCT involving the axial halide ligands. The negative A terms observed for both the intense bands for the diaqua complexes and the weaker lower energy bands for the diammine and dihydroxo complexes point out the spectroscopic accessibility of the σ^*PtO_4 orbitals b_{1g} and b_{2u}. The $(X\sigma, d\sigma) \rightarrow d\sigma^*$ excitation for the diaqua and dihalo complexes is undoubtedly at higher energy than the present measurements allow, whereas the diammine and dihydroxo complexes with stronger axial donor ligands have transitions to $(X\sigma,d\sigma)d\sigma^*$ excited states at lower energy.

Note Added in Proof. A study of the $Pt_2(SO_4)_4X_2^{n-}$, X = H_2O, Cl^-, and Br^-, ions was reported after our paper was submitted.[22] Transition assignments for the intense high-energy bands exhibited by these ions are presented which closely parallel those advanced earlier for the HPO_4^{2-} complexes[12] and involve promotion to $d\sigma^*$. These assignments should be reconsidered in light of the present MCD A-term results for these high-energy bands.

Acknowledgment is made to the NATO Scientific Affairs Division and the Middle East Technical University Research Fund for support of this work.

(22) Newman, R. A.; Martin, D. S.; Dallinger, R. F.; Woodruff, W. H.; Stiegman, A. E.; Che, C.-M.; Schaefer, W. P.; Miskowski, V. M.; Gray, H. B. *Inorg. Chem.* **1991**, *30*, 4647.

Contribution from Fuel Science Department 6211, Sandia National Laboratories, Albuquerque, New Mexico 87185, Department of Chemistry, University of New Mexico, Albuquerque, New Mexico 87131, and Department of Chemistry and Biochemistry, University of Notre Dame, Notre Dame, Indiana 46556

Effects of $\pi-\pi$ Interactions on Molecular Structure and Resonance Raman Spectra of Crystalline Copper(II) Octaethylporphyrin

L. D. Sparks,[†] W. Robert Scheidt,*[,‡] and J. A. Shelnutt*[,†]

Received November 11, 1991

Single-crystal resonance Raman measurements were performed on two crystalline phases of copper(II) octaethylporphyrin (CuOEP): triclinic A and triclinic B forms. These are compared to previously acquired resonance Raman data on the triclinic A and triclinic B phases of nickel(II) octaethylporphyrin (NiOEP). The difference in crystal packing between the triclinic A and B structures allows for more extensive $\pi-\pi$ interactions in the B form than in the A form. Differences in the single-crystal Raman spectra of the triclinic A and B forms of both Cu- and NiOEP are attributed to these $\pi-\pi$ interactions. Specifically, the Raman core-size marker lines, ν_3, ν_2, and ν_{10}, and the oxidation-state marker line, ν_4, are affected by the different packing interactions in the two crystals, and the same Raman shifting patterns between the triclinic A and B phases are observed for both Cu- and NiOEP. The metal centers exert a slight influence over the packing-induced frequency shifts in the Raman modes. Spectral results on the CuOEP crystals are also compared to solution Raman data on $\pi-\pi$ aggregated and monomeric copper(II) uroporphyrin (CuUroP). Similar to the A and B forms of NiOEP, the CuOEP triclinic A and B crystalline phases mimic the monomer and salt-induced aggregate of CuUroP in solution, as evidenced by similar magnitude upshifts in the Raman modes upon aggregation. A comparison of the structure calculated using molecular mechanics and the structure obtained from X-ray diffraction gives some insight into the effect that $\pi-\pi$ interactions have on the structure of CuOEP in the triclinic B crystal.

Introduction

The effects of $\pi-\pi$ interactions on the molecular structure and the chemical and photophysical properties of metalloporphyrins are not well understood. Stacking interactions with aromatic amino acid residues could play a role in porphyrin binding to proteins and in modulation of the chemistry and photophysics of the porphyrin cofactors. Modulation of electron-transfer rates of photosynthetic pigments and modulation of chemical properties of heme proteins are two examples. Unfortunately, few experimental methods allow definitive investigation of $\pi-\pi$ interactions between stacked porphyrin molecules or stacking interactions with aromatic residues. We are developing resonance Raman spectroscopy as a tool for the investigation and interpretation of the effects of $\pi-\pi$ interactions in stacked systems.

Previously, the crystalline forms of nickel(II) octaethylporphyrin (NiOEP) were studied by resonance Raman spectroscopy for this purpose. The three crystalline phases of NiOEP (triclinic A and B and tetragonal) were investigated,[1] and the differences in Raman spectra between the triclinic A and B phases were interpreted in

* To whom correspondence should be addressed.
[†] Sandia National Laboratories and University of New Mexico.
[‡] University of Notre Dame.

0020-1669/92/1331-2191$03.00/0